nature neuroscience

SUPPLEMENTARY INFORMATION

https://doi.org/10.1038/s41593-018-0194-1

In the format provided by the authors and unedited.

Pathogenic tau-induced piRNA depletion promotes neuronal death through transposable element dysregulation in neurodegenerative tauopathies

Wenyan Sun[1,2,3], Hanie Samimi[4], Maria Gamez[1,3], Habil Zare[3] and Bess Frost[1,3,5*]

[1]Barshop Institute for Longevity and Aging Studies, San Antonio, Texas, USA. [2]Department of Nutrition and Food Security, School of Public Health, Xi'an Jiaotong University, Xi'an, China. [3]Department of Cell Systems and Anatomy, University of Texas Health San Antonio, San Antonio, Texas, USA. [4]Department of Computer Science, Texas State University, San Marcos, Texas, USA. [5]Glenn Biggs Institute for Alzheimer's & Neurodegenerative Diseases, San Antonio, Texas, USA. *e-mail: bfrost@uthscsa.edu

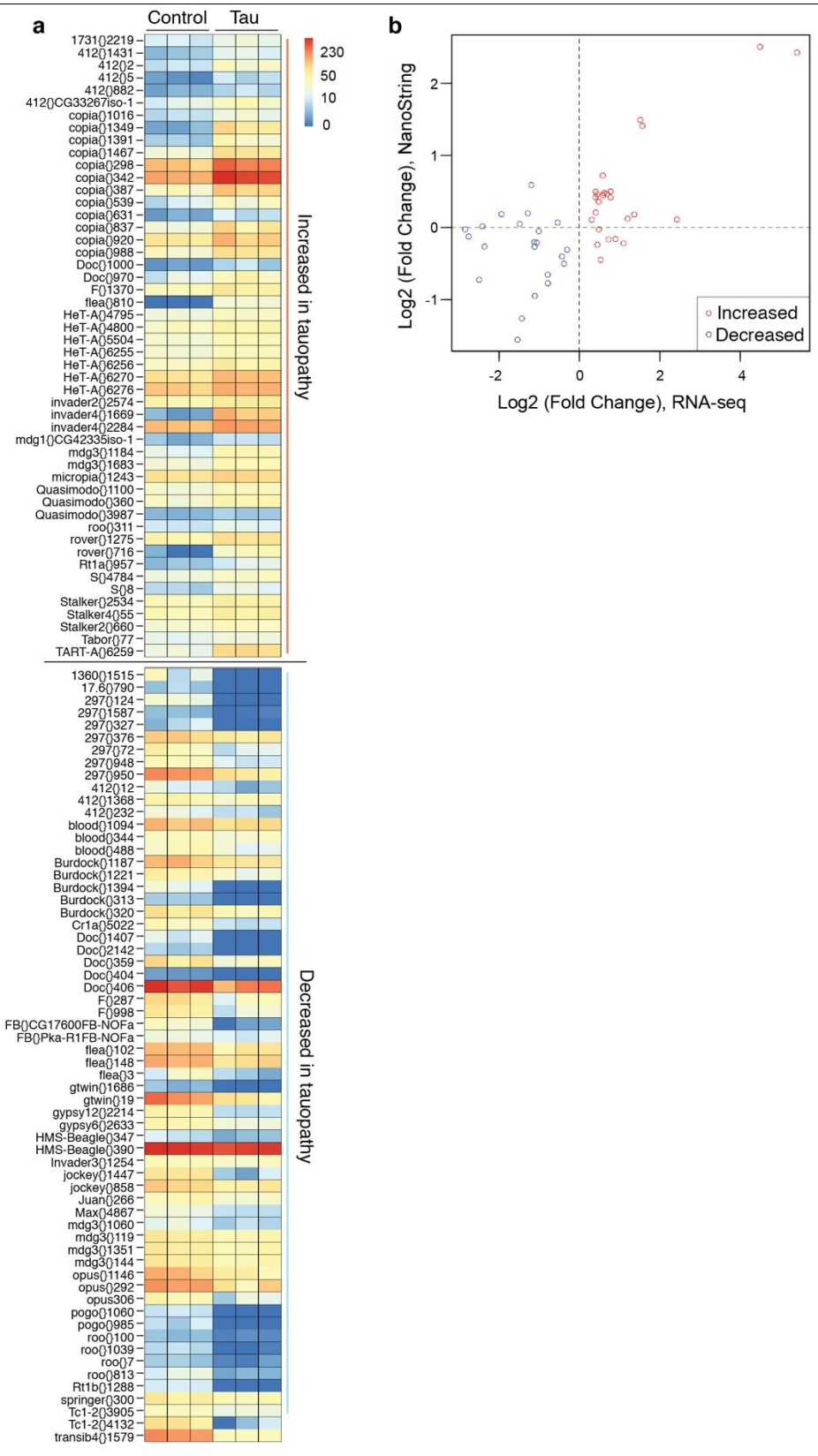

Supplementary Figure 1

Unscaled heatmaps: differentially expressed transposable element transcripts in control versus tau^{R406W} transgenic *Drosophila* based on RNA-seq.

a, Data presented in Fig. 1a, presented here as raw Transcripts Per Million (TPM). Transposable element transcripts that are differentially expressed in tau^{R406W} transgenic *Drosophila* heads versus control based on RNA-seq (two-sided Wald test, FDR, $p<0.01$, n=3 biologically independent replicates, each consisting of RNA pooled from six heads). 50 transposable elements are significantly increased at the transcript level in tau transgenic *Drosophila* compared to controls, and 60 transposable elements are significantly decreased. Transcript levels of the majority of these transposable elements are above 20 TPM in at least one of the two conditions. Supplementary Table 2 includes TPM values. **b,** Fold change measurements in RNA-seq vs. NanoString analyses. Each differentially-expressed transposable element is represented by a dot, where the colors indicate the direction of deregulation as determined based on RNA-Seq data (x-axis, n=3 biologically independent replicates). The y-axis shows the average of logarithm of fold changes measured using NanoString. The Pearson correlation between the logarithm of fold changes is 0.71 ($P<10^{-7}$), n=6 biologically independent replicates. All flies are 10 days old. Full genotypes are listed in Supplementary Table 1.

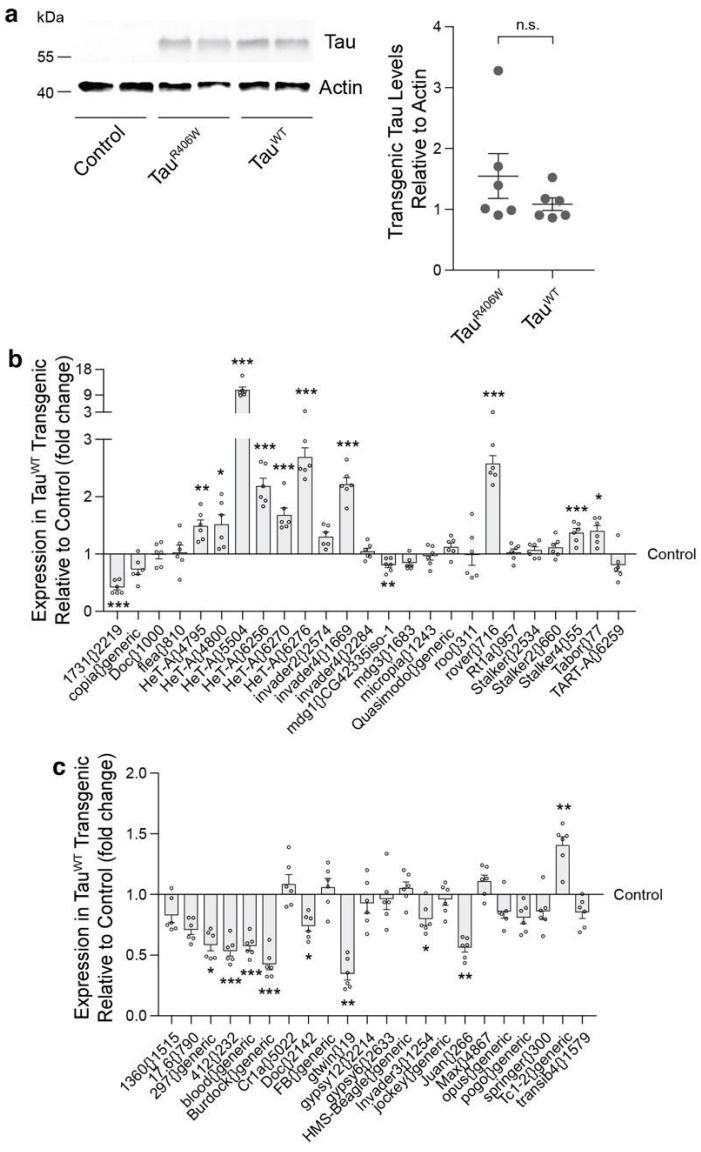

Supplementary Figure 2

Transposable element transcript levels in tau^{WT} transgenic *Drosophila.*

a, Equivalent levels of transgenic tau protein in heads of control, tau^{WT}, and tau^{R406W} transgenic *Drosophila* based on western blotting (unpaired, two-tailed Student's *t*-test, n.s.=not significant, n=6 animals per genotype). Western blot is cropped, the full blot is presented in Supplementary Fig. 10. **b**, **c,** Transposable element transcript levels in heads of tau^{WT} transgenic *Drosophila* assayed by NanoString. Transcripts that were identified as increased by RNA-seq in tau^{R406W} transgenic *Drosophila* are shown in (**b**), and transcripts that were identified as decreased by RNA-seq in tau^{R406W} transgenic *Drosophila* are shown in (**c**) (unpaired, two-tailed Student's *t*-test, **P*<0.05; ***P*<0.01; ****P*<0.001, n=6 biologically independent replicates each consisting of RNA pooled from 6 heads, values are relative to control, which was set to 1). Values are mean ± s.e.m. All flies are 10 days old. Full genotypes are listed in Supplementary Table 1. Transposable elements recognized by "generic" probes are listed in Supplementary Table 4.

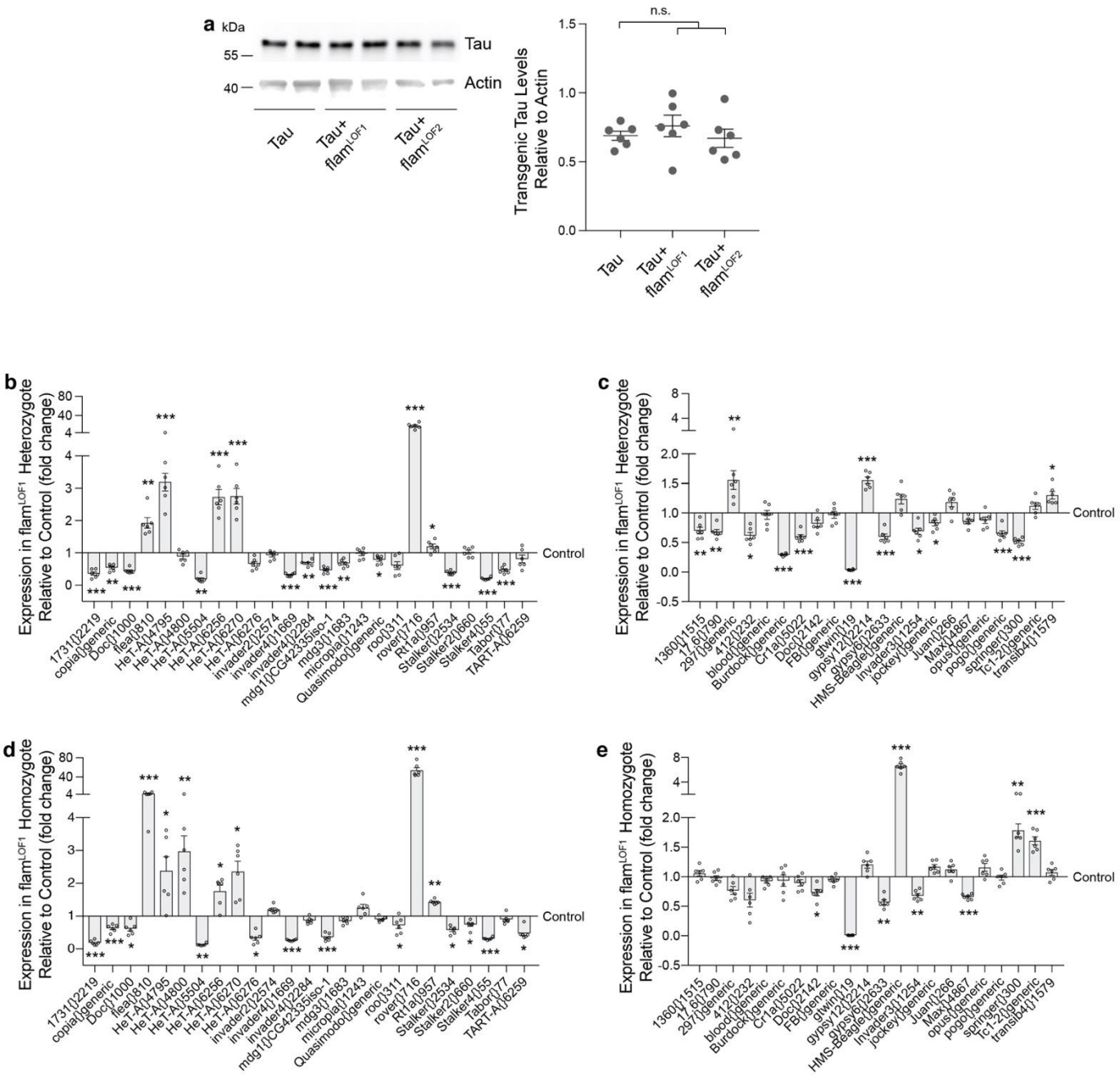

Supplementary Figure 3

Transposable element transcript levels in heads of *Drosophila* harboring a loss of function mutation in the *flamenco* locus.

a, Western blot showing equivalent levels of transgenic tau protein in heads of tau^{R406W} transgenic *Drosophila* harboring loss of function mutations in *flamenco (flam)* (unpaired, two-tailed Student's *t*-test, n.s.=not significant, n=6 animals per genotype). Western blot is cropped, the full blot is presented in Supplementary Fig. 10. **b, c,** Transposable element transcript levels in heads of *Drosophila* harboring a heterozygous loss of function mutation in the *flamenco* locus assayed by NanoString. Transcripts identified as increased by RNA-seq in tau^{R406W} transgenic *Drosophila* are shown in (**b**), and transcripts that were identified as decreased by RNA-seq in tau^{R406W} transgenic *Drosophila* are shown in (**c**). **d, e,** Transposable element transcript levels in heads of *Drosophila* harboring a homozygous loss of function mutation in the *flamenco* locus assayed by NanoString. Transcripts identified as increased by RNA-seq in tau^{R406W} transgenic *Drosophila* are shown in (**d**), and transcripts that were identified as decreased by RNA-seq in tau^{R406W} transgenic *Drosophila*

are shown in (**e**). Unpaired, two-tailed Student's *t*-test, **P*<0.05; ***P*<0.01; ****P*<0.001. For **b-e**, n=6 biologically independent replicates each consisting of RNA pooled from 6 heads, values are relative to control, which was set to 1. Values are mean ± s.e.m. All flies are 10 days old. Full genotypes are listed in Supplementary Table 1. Transposable elements recognized by "generic" probes are listed in Supplementary Table 4.

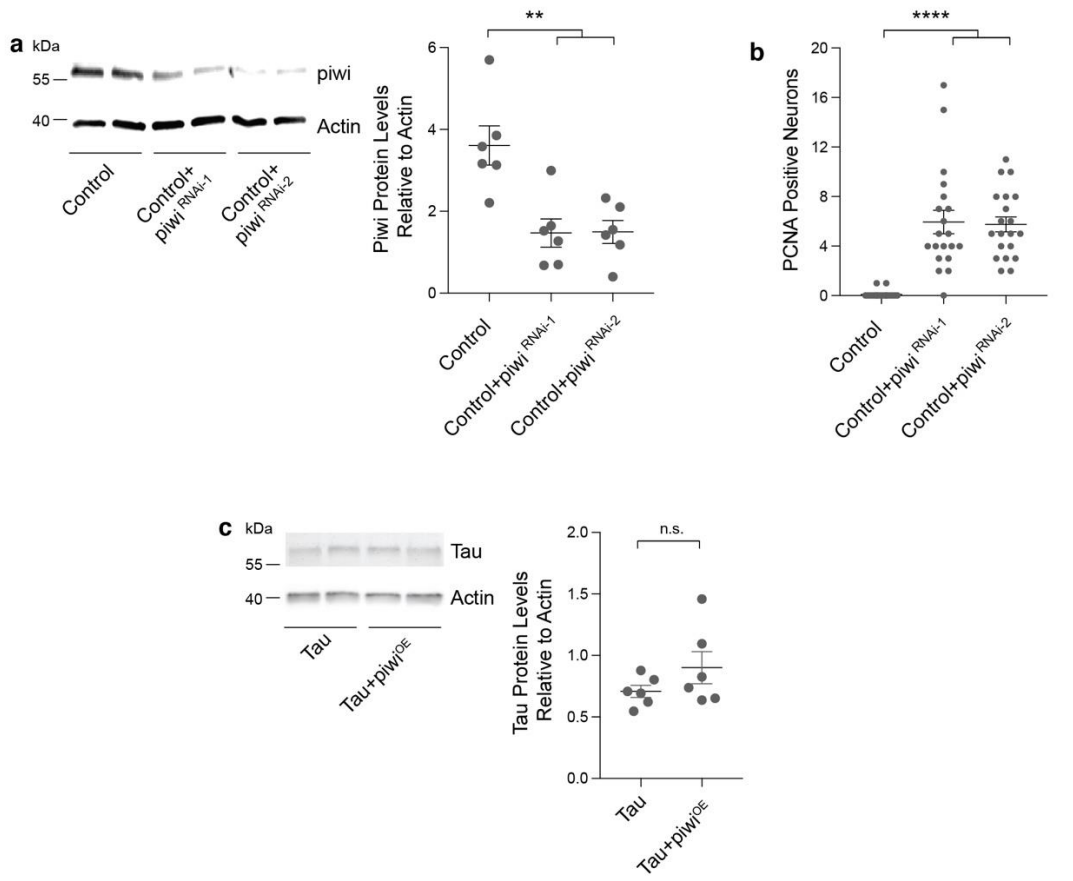

Supplementary Figure 4

Genetic manipulation of *piwi*.

a, Total levels of piwi protein in whole head homogenates from *Drosophila* harboring RNAi transgenes targeting *piwi* (one-way ANOVA with Tukey's multiple comparison test, $^{**}P<0.01$, n=6 animals per genotype). **b,** Cell cycle activation assayed by PCNA staining in brains of *Drosophila* harboring RNAi transgenes targeting *piwi* (one-way ANOVA with Tukey's multiple comparison test, $^{****}P<0.0001$, n=20 animals per genotype). **c**, Total transgenic tau levels in whole head homogenates from tau^{R406W} transgenic *Drosophila* with and without pan-neuronal overexpression of piwi (unpaired, two-tailed Student's *t*-test, n.s.=not significant, n=6 animals per genotype). Values are mean ± s.e.m. All flies are 10 days old. Western blots are cropped in **a** and **c**, full blots are presented in Supplementary Fig. 10. Full genotypes are listed in Supplementary Table 1.

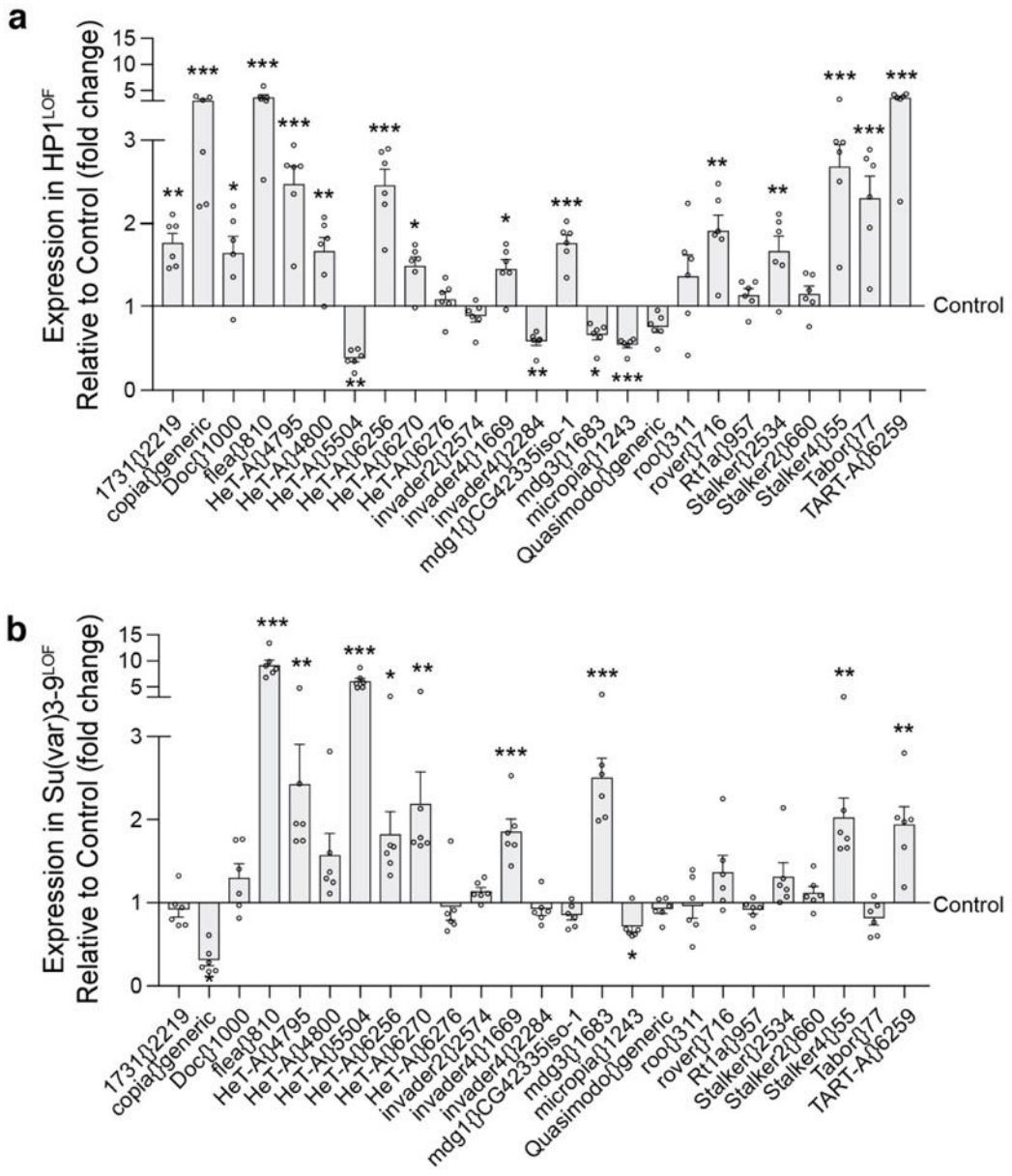

Supplementary Figure 5

Heterochromatin decondensation increases levels of transposable element transcripts in *Drosophila* heads.

NanoString analysis of transposable element transcript levels in *Drosophila* harboring a loss of function mutation in *Su(var)205* shown in **a**, *or Su(var)3-9* shown in **b** (unpaired, two-tailed Student's *t*-test, **P*<0.05, ***P*<0.01, ****P*<0.001, n=6 biologically independent replicates each consisting of RNA pooled from 6 heads, values are relative to control, which was set to 1). Values are mean ± s.e.m. All flies are 10 days old. Full genotypes are listed in Supplementary Table 1. Transposable elements recognized by "generic" probes are listed in Supplementary Table 4.

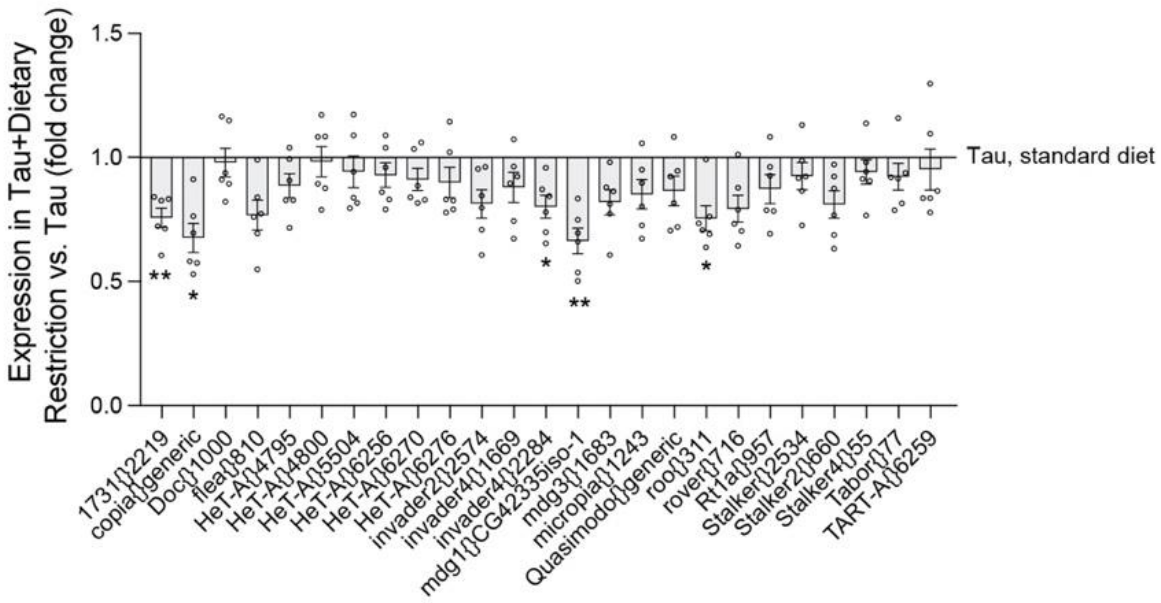

Supplementary Figure 6

Transposable element transcript levels in tau transgenic *Drosophila* in response to dietary restriction.

Transposable element transcript levels in tau^{R406W} transgenic *Drosophila* with 66% dietary restriction assayed by NanoString (unpaired, two-tailed Student's *t*-test, **P*<0.05, ***P*<0.01, n=6 biologically independent replicates each consisting of RNA pooled from 6 heads, values are relative to tau^{R406W} fed a standard diet, which was set to 1). Values are mean ± s.e.m. All flies are 10 days old. Full genotypes are listed in Supplementary Table 1. Transposable elements recognized by "generic" probes are listed in Supplementary Table 4.

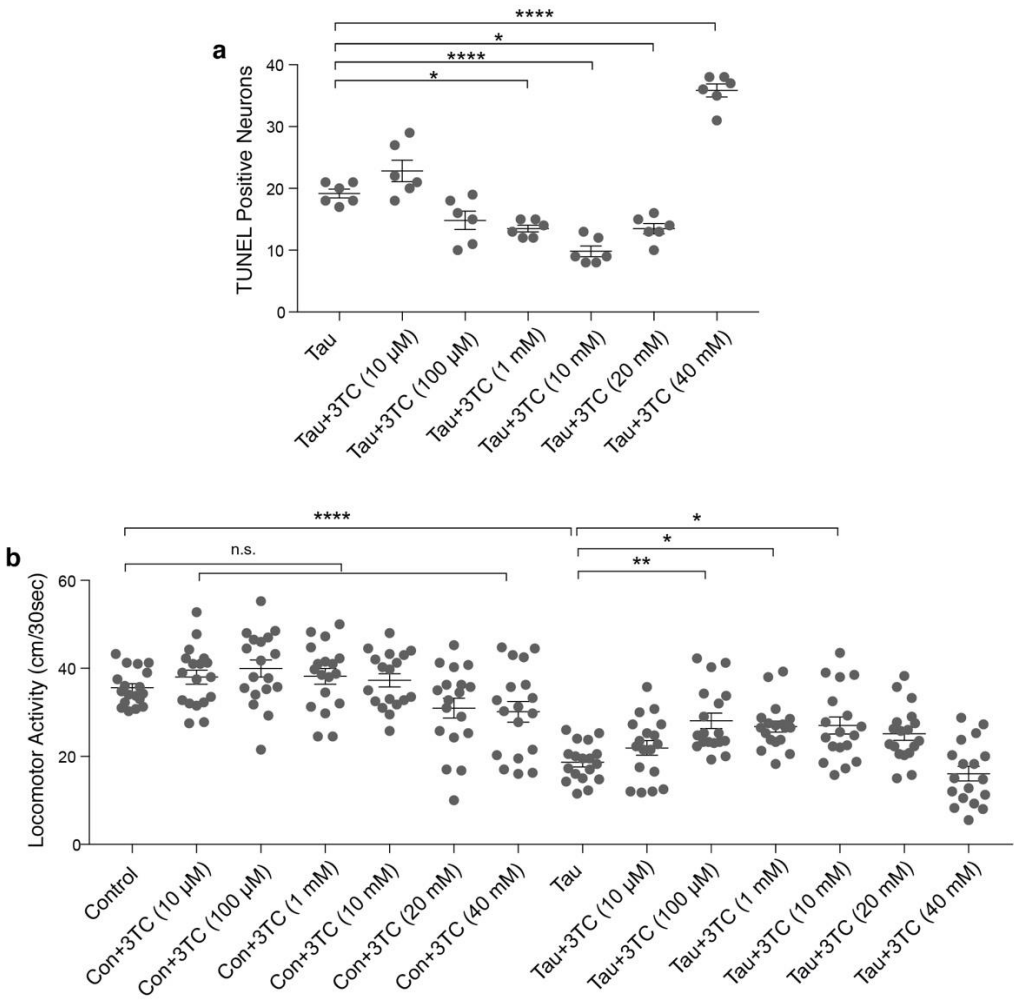

Supplementary Figure 7

Dose-response of 3TC treatment.

a, Neuronal death assayed by TUNEL in tau^{R406W} transgenic *Drosophila* treated with the indicated dose of 3TC (unpaired, two-tailed Student's *t*-test, **P*=0.0157, *****P*<0.0001, n=6 animals per treatment). **b**, Locomotor activity in control and tau^{R406W} transgenic *Drosophila* treated with the indicated dose of 3TC (one-way ANOVA with Tukey's multiple comparison test, n.s.=not significant, **P*<0.05, ***P*=0.0077, *****P*<0.0001, n=18 animals per genotype, per treatment). Values are mean ± s.e.m. All flies are 10 days old. Full genotypes listed in Supplementary Table 1.

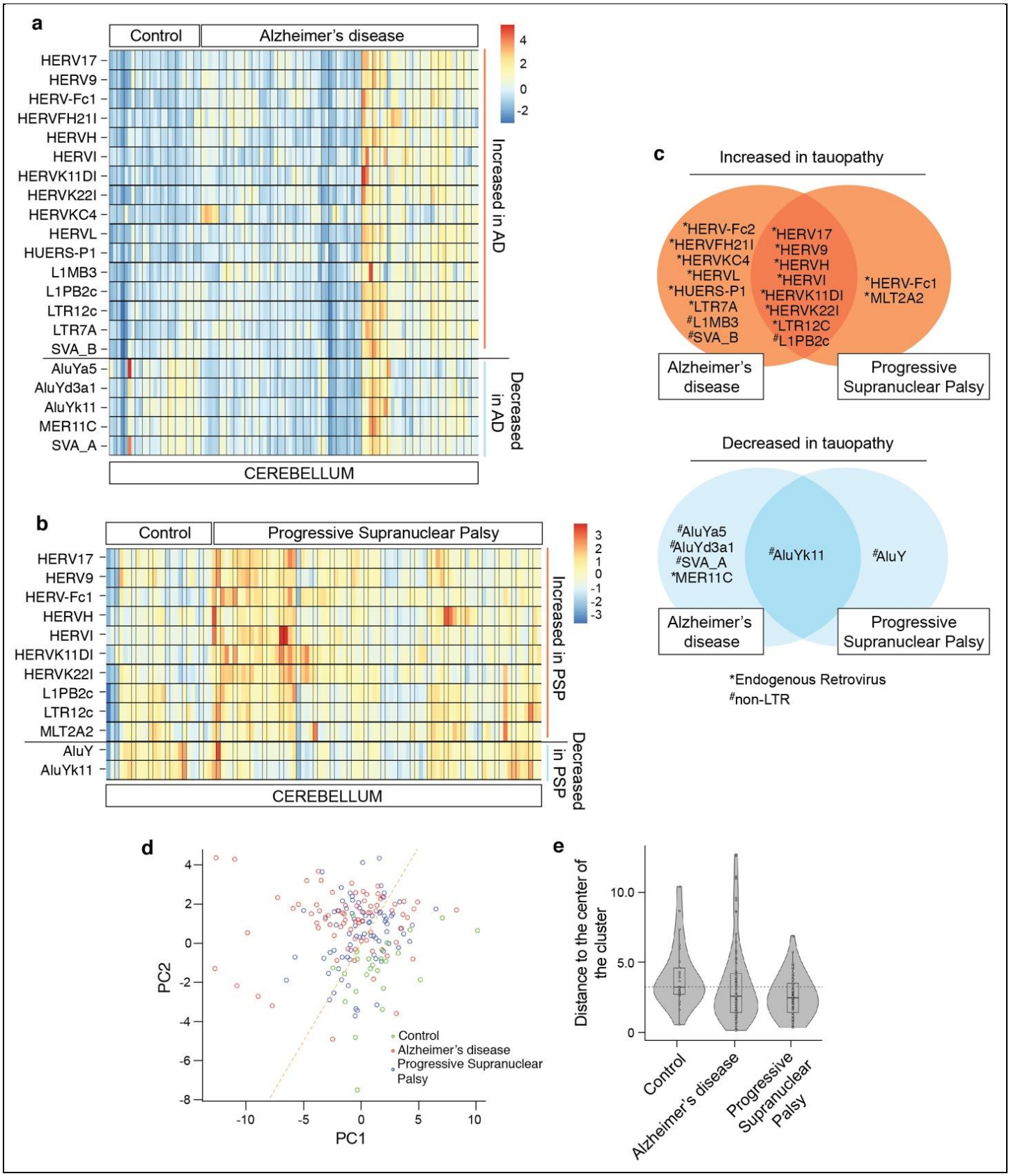
a
Control
Alzheimer's disease
HERV17
HERV9
HERV-Fc1
HERVFH21I
HERVH
HERVI
HERVK11DI
HERVK22I
HERVKC4
HERVL
HUERS-P1
L1MB3
L1PB2c
LTR12c
LTR7A
SVA_B
AluYa5
AluYd3a1
AluYk11
MER11C
SVA_A
Increased in AD
Decreased in AD
CEREBELLUM
4
2
0
-2
b
Control
Progressive Supranuclear Palsy
HERV17
HERV9
HERV-Fc1
HERVH
HERVI
HERVK11DI
HERVK22I
L1PB2c
LTR12c
MLT2A2
AluY
AluYk11
Increased in PSP
Decreased in PSP
CEREBELLUM
3
2
1
0
-1
-2
-3
c
Increased in tauopathy
*HERV-Fc2
*HERVFH21I
*HERVKC4
*HERVL
*HUERS-P1
*LTR7A
#L1MB3
#SVA_B
*HERV17
*HERV9
*HERVH
*HERVI
*HERVK11DI
*HERVK22I
*LTR12C
#L1PB2c
*HERV-Fc1
*MLT2A2
Alzheimer's disease
Progressive Supranuclear Palsy
Decreased in tauopathy
#AluYa5
#AluYd3a1
#SVA_A
*MER11C
#AluYk11
#AluY
Alzheimer's disease
Progressive Supranuclear Palsy
*Endogenous Retrovirus
#non-LTR
d
PC2
PC1
4
2
0
-2
-4
-6
-8
-10
-5
0
5
10
Control
Alzheimer's disease
Progressive Supranuclear Palsy
e
Distance to the center of the cluster
10.0
5.0
0
Control
Alzheimer's disease
Progressive Supranuclear Palsy

Supplementary Figure 8

Transposable element transcript levels in cerebellum of human tauopathy.

Heatmaps reflecting fold change of differentially expressed transposable element transcripts in human cerebellum in **a**, control versus Alzheimer's disease (AD), and **b**, control versus progressive supranuclear palsy (PSP), based on RNA-seq (two-sided Wald test, FDR, $P<0.01$). **c,** Differentially expressed transposable elements in postmortem Alzheimer's disease and progressive supranuclear palsy cerebellum. HERVs are significantly over-represented among transposable elements that are increased in tauopathy (hypergeometric test, adjusted $P=0.0003$). Non-LTR are significantly over-represented among transposable elements that are decreased in tauopathy (hypergeometric test, adjusted $P=0.01$). **d,** Principal component analyses of differentially expressed transposable elements in control, Alzheimer's disease, and progressive supranuclear palsy cerebellum (Kolmogorov-Smirnov test, $P<10^{-14}$). **e,** Violin plots show that control samples are relatively farther from the center of the cluster, defined as the median of tauopathy cerebellum samples. Euclidian distance was computed using the two first principal components of those transposable elements that are differentially expressed among the three conditions. For control, AD, and PSP respectively, minima=0.5, 0.08, 0.3, maxima=10.4, 12.7, 6.9, median=3.1, 2.5, 2.4, mean=4.0, 3.4, 2.6, 1^{st} quantile=2.7, 1.4, 1.4, 3^{rd} quantile=4.6, 4.2, 3.5. Control n=25, Alzheimer's disease n=76, progressive supranuclear palsy n=78 biologically independent replicates in **a**-**e**.

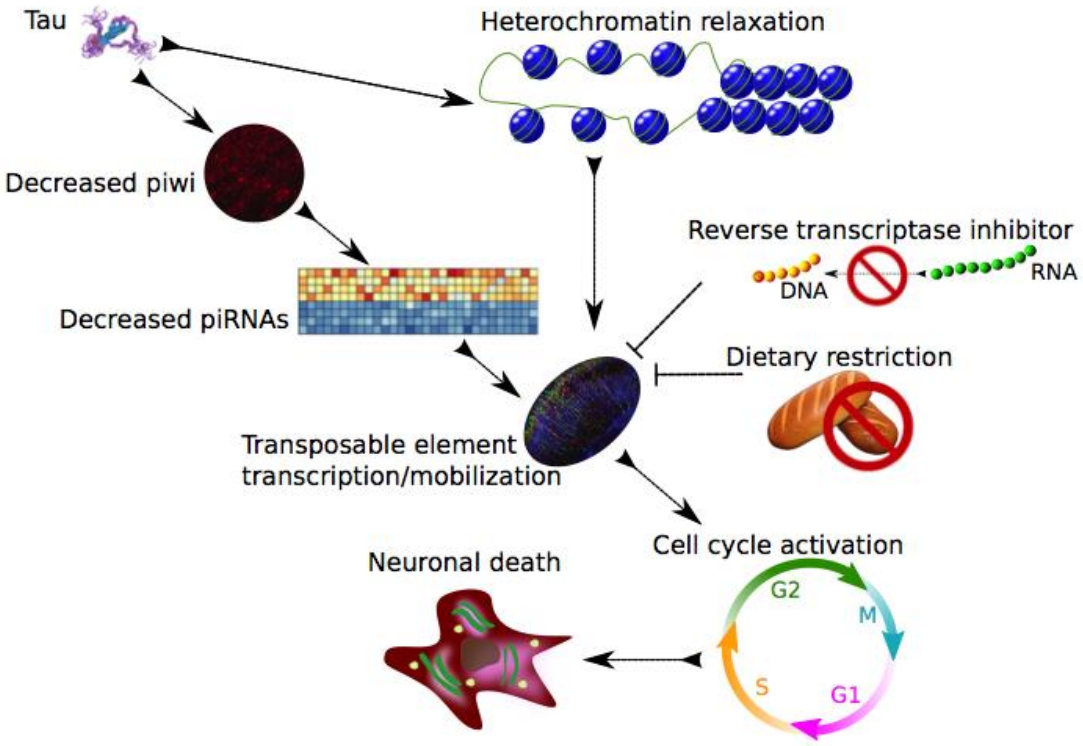

Supplementary Figure 9

Graphical summary.

Pathological tau disrupts heterochromatin- and piRNA-mediated transposable element silencing. Activation of transposable elements promotes aberrant activation of the cell cycle in post-mitotic neurons, which is sufficient to induce neuronal death. A nucleoside analog inhibitor of reverse transcriptase, 3TC, as well as dietary restriction suppress transposable element dysregulation in tauopathy, and decrease tau-induced neurotoxicity.

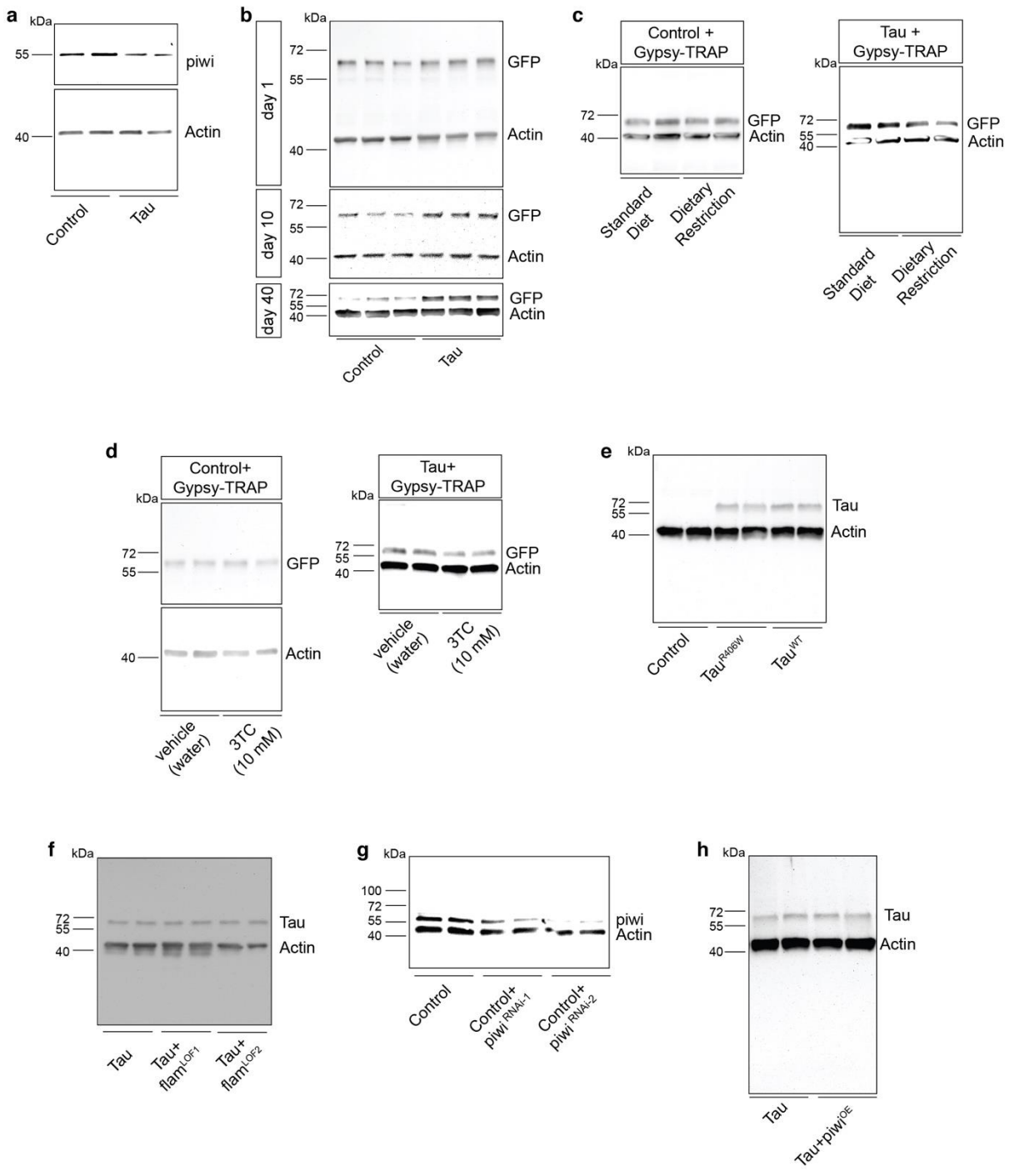

Supplementary Figure 10

Full scans of western blots.

a) Western blot from Fig. 3c. **b)** Western blot from Fig. 4b. **c)** Western blots from Fig. 5b. **d)** Western blots from Fig. 6b. **e)** Western blot from Supp. Fig. 2a. **f)** Western blot from Supp. Fig. 3a. **g)** Western blot from Supp. Fig. 4a. **h)** Western blot from Supp. Fig. 4c.

Name in the manuscript	**Full Genotype**
Control	*elav-GAL4/+*
Tau^{R406W}	*elav-GAL4/+;UAS-Tau^{R406W}/+*
Tau^{WT}	*elav-GAL4/+;UAS-Tau^{WT}/+*
Control+Gypsy-TRAP	*ovo-GAL80/+;GMR-GAL4/+;UAS-GFP/+*
Tau+Gypsy-TRAP	*ovo-GAL80/+;GMR-GAL4/+;UAS-GFP/GMR-Tau^{V337M}*
Control+$piwi^{RNAi-1}$	*elav-GAL4/+;UAS-piwi^{v101658}/+*
Control+$piwi^{RNAi-2}$	*elav-GAL4/+;UAS-piwi^{v22235}/+*
Control+$piwi^{OE}$	*elav-GAL4/+;UAS-HA-piwi/+*
Control+$flam^{LOF1}$	*elav-GAL4/flam^{OR}*
Control+$flam^{LOF2}$	*elav-GAL4/flam^{KG00476}*
Tau+$flam^{LOF1}$	*elav-GAL4/flam^{OR};UAS-Tau^{R406W}/+*
Tau+$flam^{LOF2}$	*elav-GAL4/flam^{KG00476};UAS-Tau^{R406W}/+*
Tau+$piwi^{OE}$	*elav-GAL4/+;UAS-HA-piwi/+;UAS-Tau^{R406W}*
Su(var)3-9^{LOF}	*elav-GAL4/+;Su(var)3-9^{2}/+*
$HP1^{LOF}$	*elav-GAL4/+;Su(var)205^{5}/+*

Supplementary Table 1 | Full *Drosophila* Genotypes.

(Included as an Excel spreadsheet)

Supplementary Table 2 | Differential expression analysis of transposable elements in *Drosophila* based on RNA-seq. The first column includes the FlyBase IDs of transposable elements, which are ordered based on *P*-values. The next six columns, computed using DESeq2, are: the mean of the normalized counts (basemean), the logarithm of the fold change (log2FoldChange), the standard error of the log2FoldChange (lfcSE), the two-sided Wald statistic defined as the log2FoldChange divided by lfcSE (stat), the *P*-value of the Wald test, and the Benjamini-Hochberg adjusted *P*-value (padj). The raw counts from RNA-seq are also included.

(Included as an Excel spreadsheet)

Supplementary Table 3 | Sequences of NanoString probes.

Generic Probe	Elements Recognized by Generic Probe
297{}generic	*297{}72* *297{}327* *297{}376* *297{}950*
blood{}generic	*blood{}344* *blood{}488* *blood{}1094*
Burdock{}generic	*Burdock{}1187* *Burdock{}1221*
copia{}generic	*copia{}298* *copia{}342* *copia{}387* *copia{}539* *copia{}631* *copia{}837* *copia{}920* *copia{}988* *copia{}1016* *copia{}1349* *copia{}1391* *copia{}1467*
FB{}generic	*FB{}CG17600$^{FB\text{-}NOF}$a* *FB{}Pka-R1$^{FB\text{-}NOF}$a*
HMS-Beagle{}generic	*HMS-Beagle{}347* *HMS-Beagle{}390*
jockey{}generic	*jockey{}858* *jockey{}1447*
opus{}generic	*opus{}292* *opus{}306* *opus{}1146*
pogo{}generic	*pogo{}985* *pogo{}1061*
Quasimodo{}generic	*Quasimodo{}360* *Quasimodo{}1100*
Tc1-2{}generic	*Tc1-2{}3905* *Tc1-2{}4132*

Supplementary Table 4 | Transposable elements recognized by "generic" NanoString probes.

(Included as an Excel spreadsheet)

Supplementary Table 5 | Differential expression analysis of piRNAs in *Drosophila*. The first column is the piRNA name sorted by *P*-value (two-sided Wald test), and the next six columns are similar to Supplementary Table 2, which is described above. In addition to raw counts, the sum of counts in each condition is included, as well as the ratio of the sum of the counts in tau transgenic samples over the sum of the counts in control samples. Because a piRNA can have multiple copies in the *Drosophila* genome, we included the number of copies (frequency) and their genomic locations, which are separated using a "*". The last column is the sequence of the piRNA.

(Included as an Excel spreadsheet)

Supplementary Table 6 | Genomic locations of *Drosophila* piRNAs. The first column is the piRNA name sorted by *P*-value of two-sided tests. The chromosome, start, end, strand, sequence, number of copies (frequency), and the adjusted *P*-value from the small RNA-seq data are included. n=4 biologically independent replicates of each genotype, each consisting of RNA pooled from 6 heads. *P* values were calculated based on a two-sided Wald test, FDR.

(Included as an Excel spreadsheet)

Supplementary Table 7 | Differential expression of transposable elements in human tauopathy. In each of the first six sheets, the transposable elements are sorted based on the *P*-value corresponding to the tissue (cortex or cerebellum) and the condition specified in the sheet name. Columns are similar to Supplementary Table 2. The last two sheets are the clinical data including the diagnosis and the RIN of RNA samples. More detail on clinical information, including gender, age at death, apolipoprotein E (ApoE), sequencing flow cell batch, and post mortem interval is available at the Synapse.org website (cortex: http://dx.doi.org/10.7303/syn5223705.3, cerebellum: http://dx.doi.org/10.7303/syn3817650.6). *P* values were calculated based on a two-sided Wald test, FDR.

Antibody	Western Blotting	Immunostaining	Source
Actin	1:50,000		Abcam #ab8227
GFP	1:1,000		UCDavis/NIH NeuroMab #75-131
PCNA		1:200	Dako #M0879
piwi	1:500	1:50	Abcam #5207
cTau	1:2,000,000	1:10,000	Dako #A0024
Alexa555-conjugated secondary (rabbit)		1:200	Life Technologies #A21424
Biotin-conjugated secondary (rabbit)		1:200	Southern Biotech #4010-08
HRP-conjugated secondary (mouse)	1:10,000		Southern Biotech #1010-05
HRP-conjugated secondary (rabbit)	1:1,000		Southern Biotech #3010-05

Supplementary Table 8 | Antibody information.

(Included as an Excel spreadsheet)

Supplementary Table 9 | Statistical Analyses.